

Efficient parameterization of transferable Atomic Cluster Expansion for water

Eslam Ibrahim,* Yury Lysogorskiy,* and Ralf Drautz*

ICAMS, Ruhr Universität Bochum, 44780 Bochum, Germany

E-mail: eslam.saadibrahim@rub.de; yury.lysogorskiy@rub.de; ralf.drautz@rub.de

Abstract

We present a highly accurate and transferable parameterization of water using the atomic cluster expansion (ACE). To efficiently sample liquid water, we propose a novel approach that involves sampling static calculations of various ice phases and utilizing the active learning (AL) feature of ACE-based D-optimality algorithm to select relevant liquid water configurations, bypassing computationally intensive ab-initio molecular dynamics (AIMD) simulations. Our results demonstrate that the ACE descriptors enable a potential initially-fitted solely on ice structures which is later upfitted with few configurations of liquid, identified with active learning to provide an excellent description of liquid water. The developed potential exhibits remarkable agreement with first-principles reference, accurately capturing various properties of liquid water, including structural characteristics such as pair correlation functions, covalent bonding profiles, and hydrogen bonding profiles, as well as dynamic properties like the vibrational density of states, diffusion coefficient and thermodynamic properties such as the melting point of the ice Ih. Our research introduces a new and efficient sampling technique for machine learning potentials in water simulations, while also presenting a transferable interatomic potential for water that reveals the accuracy of first principles reference. This advancement not only enhances our understanding the relationship between ice and liquid water at the atomic level, but also opens up new avenues for

studying complex aqueous systems.

1 Introduction

Understanding and predicting the properties of water is crucial for numerous fields, including chemistry, materials science, and biology.^{1,2} Despite the simplicity of the H₂O molecule, the simulation of molecular-level dynamics of water and its phases³⁻⁶ remains challenging due to the presence of strong intermolecular interactions.⁷⁻¹² The choice of ab-initio functionals significantly impacts simulation outcomes¹³⁻¹⁵ and several investigations were carried out to evaluate predictions of water properties.¹³⁻²³

Ice in its various crystalline forms exhibits a wide range of structural motifs, each characterized by a specific arrangement of water molecules. Liquid water, on the other hand, lacks long-range order but forms transient hydrogen bonds, which leads to close similarities in structure between ice and water.²⁴ Understanding the relation between the atomic structure of different ice phases and liquid water is crucial for unraveling the intricate structure-property relationships that govern the properties of water.³

Experiments such as X-ray diffraction²⁵ and infrared spectroscopy^{26,27} have provided fundamental insight into the atomic structure of ice and liquid water. Atomic scale analysis is challenging²⁸⁻³³ and computational approaches, particularly molecular dynamics simulations, have emerged as a powerful tool to complement experimental studies. Empirical models and in-

teratomic potentials led the way.^{34–37}

In recent years, machine learned interatomic potentials have enabled much more accurate predictions^{38–40} and a substantial number of machine learned interatomic potentials for liquid water were developed.^{3–5,41–48}

We present a highly accurate and transferable parameterization for ACE that we demonstrate captures the intricacies of water atomic interactions with the accuracy of the first-principles reference. Different from most other MLPs, we do not base our parameterization on data obtained from ab initio molecular dynamics simulations in water. Instead, we exploit the fact that the local atomic motifs present in liquid water can also be obtained from ice with displaced atomic positions, which provides a more efficient parameterization strategy.

The remainder of this article is organized as follows: Section 2 provides an overview of the computational methods employed in this study. Section 3 focuses on the relation between ice phases and liquid water together with a various validation tests. Finally, Section 4 summarizes the key results and discusses their implications for future studies in the field of water science.

2 Methods

2.1 Reference calculations

We utilized the Vienna Ab initio Simulation Package (VASP)^{49–51} for conducting density functional theory (DFT) calculations. All DFT calculations were performed employing the Perdew-Burke-Ernzerhof (PBE) exchange-correlation functional.⁵² To account for van der Waals (vdW) dispersion interactions, we incorporated the Grimme D3 method,^{53,54} where earlier studies had shown that it benefits from intrinsic functional error cancellations,¹⁸ leading to a description of water that compares very well with experiment in simulations with classical nuclei. A k-mesh density of $0.125/\text{\AA}$, a plane wave energy cutoff of 450 eV.

The initial set of 83 ice structures were fully relaxed, for all other configurations that were generated using active learning energies and

forces were calculated solely in static calculations.

2.2 Molecular dynamics simulations

The Large-scale Atomic/Molecular Massively Parallel Simulator (LAMMPS)⁵⁵ with the MLPACE pair style⁵⁶ were employed to carry out molecular dynamics (MD) simulations. The vibrational density of states (VDOS) were obtained from the velocity auto-correlation function (VACF) as implemented in i-pi.⁵⁷

2.3 Atomic cluster expansion

ACE^{58,59} training was carried out using the package Pacemaker.⁶⁰ We employed a Finnis-Sinclair-type mildly non-linear representation of the atomic energy that incorporates two atomic properties, which are represented by linear ACE basis expansions.^{56,58,60} The non-linear representation is motivated by the second-moment approximation and has been demonstrated to be efficient for metals^{56,60,61} as well as covalently bonded materials,^{62,63} for non-collinear magnetic degrees of freedom,⁶⁴ message passing⁶⁵ and ACE-based graph basis functions.⁶⁶

2.4 Training dataset

2.4.1 Generation of diverse ice phases

We started by generating a diverse set of structures using the genice code,^{67,68} which implements a graph-theory based algorithm to ensure topological characteristics of proton-ordered as well as proton-disordered ice. We selected initially 83 ice structures with up to 310 atoms for training a first ACE, where we adopt the same naming convention from the genice code. Using this ACE, we used active learning⁶⁹ to select further ice structures with densities from 0.1 to 17 g/mL and with random deformations on atomic positions and cell. The dataset for training was obtained by constraining maximum force components to below 35 eV/ \AA and densities from 0.16 to 1.82 g/mL.

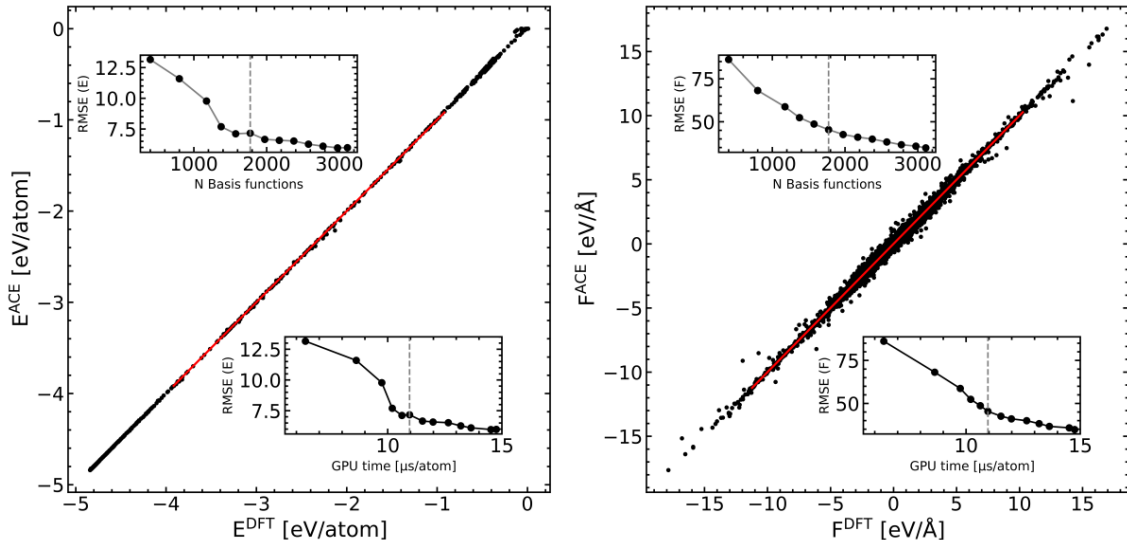


Figure 1: Comparison of ACE predictions for energies and forces to DFT reference. Insets show the convergence of RMSE with respect to the number of ACE basis functions and the GPU time in units of eV/atom and eV/Å, respectively for NVIDIA GeForce RTX 3060 Ti (compute architecture 8.6).

2.4.2 Generation of liquid configurations using active learning

To avoid computationally expensive ab-initio molecular dynamics (AIMD) simulations for sampling liquid water, we ran molecular dynamics in the isobaric-isothermal ensemble (NPT) with the ACE that was trained solely on ice structures (ACE-ice). During the simulation we kept track of the uncertainty indicator⁶⁹ to identify extrapolative configurations, from which we selected some for DFT calculations.

2.5 Training procedure

For ACE parameterization we employed a successive hierarchical basis extension with power-order ranking of basis functions⁶⁰ up to body order five and a cutoff of 6.0 Å. We started training from the 83 initial ice structures, where we include the first and last configuration from the full ionic relaxation in addition to 5 deformed configurations for every structure. This resulted in 581 structures with 49686 atoms. In a first active learning step, we generated more deformed ice structures with a wider range of densities and further added O-O, H-H and O-H dimers to the training data. This dataset comprised 2432 structures with 155068

atoms. In the second and final active learning step, we used ACE in molecular dynamics simulations at various NPT conditions and selected liquid configurations with large extrapolation grades. This resulted in a final dataset of 2575 structures and 173686 atoms. We summarize the steps in Table. 1.

Table 1: Different active learning steps for dataset generation.

| AL step | Type | N configurations | N atoms |
|---------|--------------------------|------------------|---------|
| 0th | Initial ices | 581 | 49686 |
| 1st | Highly deformed ices | 2335 | 157174 |
| 2nd | O-O, O-H and H-H dimers | 2432 | 155068 |
| 3rd | AL-selected liquid water | 2575 | 173686 |

Energies and forces were weighted in the loss function using an energy based weighting scheme⁶⁰ that gave higher weights to low energy structures. We truncated the expansion at 1774 basis functions with 4844 parameters. This resulted in a parameterization of mean-absolute-error (MAE) for energies of 2.5 meV/atom and MAE for forces of 16.7 meV/Å⁻¹. Fig. 1 shows that ACE reproduces the DFT reference data with excellent accuracy and illustrates that we truncated the expansion as a compromise between accuracy and computational cost.

2.6 ACE-map

We utilize the ACE basis functions directly to examine the local atomic environments in ice and liquid water. We employ t-distributed Stochastic Neighbor Embedding (t-SNE)^{70,71} as implemented in Scikit-learn⁷² to reduce the dimensionality of basis function space for local atomic environments of hydrogen and oxygen. The input data consisted of all basis functions for all structures from the 2nd active learning step alongside selected liquid structures at 300 K. Our approach is similar to Ref.,³ but differently we employ the non-linear t-SNE algorithm, which helps to maintain local structure.

3 Results

3.1 ACE-map for water

Solid and liquid atomic environments overlap in ACE-map Fig. 2. This coincides with the observation from Ref.³ that liquid water contains the building blocks of ice. Here we turn this around. Ice phases including atomic displacements contain the structural motifs of liquid water. This leads us to an efficient parameterization strategy. Instead of generating a training database for liquid water from computationally expensive AIMD that requires many time steps to de-correlate atomic configurations, we employ solid ice phases with randomly displaced atomic positions. These structures are immediately de-correlated and automatically significant for the simulation of water.

Furthermore, our selection of ice phases ensures dense coverage of the PES, enabling our potential to avoid falling into sparsely sampled regions of the trained PES. This approach also facilitates stable molecular dynamics simulations of liquid water using ACE-ice without prior fitting. Consequently, we efficiently identify crucial liquid configurations based on extrapolation.⁶⁹

3.2 Energy-volume curves for ice phases

In Fig. 3, we show energy as a function of volume for a number of different ice phases. The DFT calculations marked by red crosses were used for validation only. The panels demonstrate excellent transferability of ACE between a wide variety of different ice structures.

3.3 Correlation and bonding profiles

We compute various pair correlation functions and profiles for different types of bonding in liquid water employing both ACE and DFT. Specifically, we analyze the radial distribution functions (RDFs) for H-H, O-H, and O-O distributions in liquid water at a density of 0.99709 g/mL and temperature of 298 K. Our simulations utilize a cell containing 256 molecules, simulated over 100 ps across 7 independent runs, totaling 700 ps with an adapted pyiron⁷³ implementation of neighbour lists. The choice of system size is guided by prior studies, indicating convergence of correlation functions with 128 molecules.⁴⁴ Comparison with DFT reference data, depicted in Fig. 4, demonstrates excellent agreement of our ACE parameterization with the radial distribution functions from DFT. In particular, for validation, DFT results are obtained from simulations comprising 64 water molecules equilibrated over 1 ps, followed by a 7 ps production run, where none of these DFT configurations are included in our training dataset. While DFT results exhibit more noise compared to ACE simulations due to shorter simulation time, our AIMD data aligns with previous findings.¹⁹

Prior studies have highlighted the efficacy of the revPBE-D3 functional in describing O-O RDF compared to experimental results via classical MD simulations.^{19,44} The discrepancy between quantum simulations and classical predictions is attributed to the cancellation of errors present in classical simulations but absent in quantum simulations. Notably, meta-GGA functionals offer improved descriptions in quantum simulations.^{19,41,43,44,74}

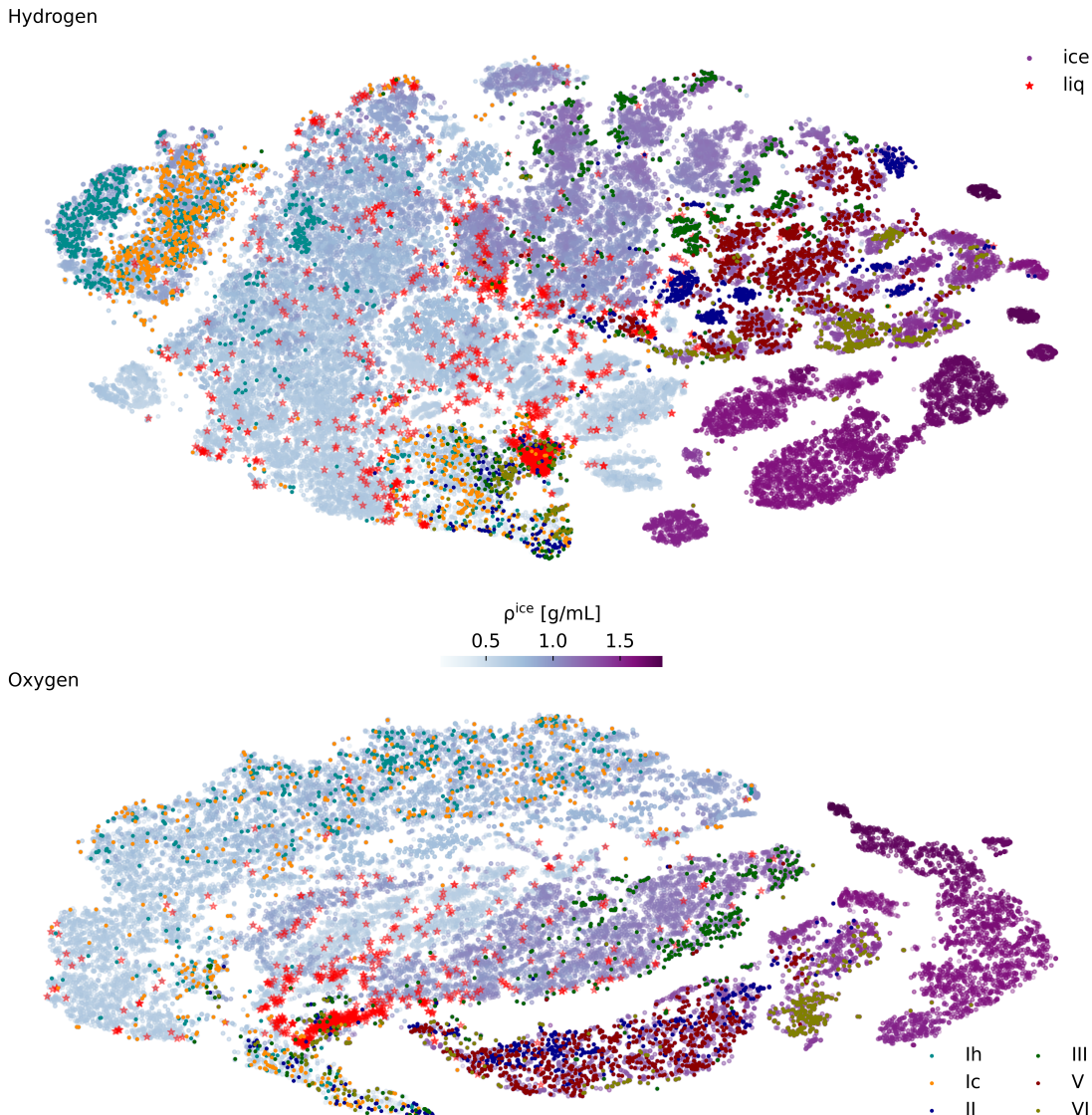


Figure 2: T-SNE maps of ice phases and water configurations at 300 K. Hydrogen and oxygen environments are characterized separately (top and bottom, respectively). Red stars indicate environments in liquid configurations, while dots of different colors mark different ice phases, including atomic displacements in these phases. Light to bold color indicate increasing density.

We further present bonding profiles for both covalent O-H bonds and hydrogen bonds. Covalent O-H bonds involve hydrogen and oxygen atoms within the same molecule, while hydrogen bonds form between a hydrogen atom of one molecule and an oxygen atom of another, as illustrated in Fig. 4. Our ACE parameterization consistently provides accurate predictions for both types of bonds compared to DFT.

3.4 Vibrational density of states

In Fig. 5, we show the vibrational density of states for liquid water (VDOS) at 300 K. We calculate the VDOS from Fourier transform of the VACF $c_{vv}(\omega)$, as implemented in the i-PI engine,

$$c_{vv}(\omega) = \int \langle \nu(\tau)\nu(\tau+t) \rangle_{\tau} e^{-i\omega t} dt. \quad (1)$$

Our predictions compare well to experimental data⁷⁵ that is shown by vertical dashed lines in Fig.5.

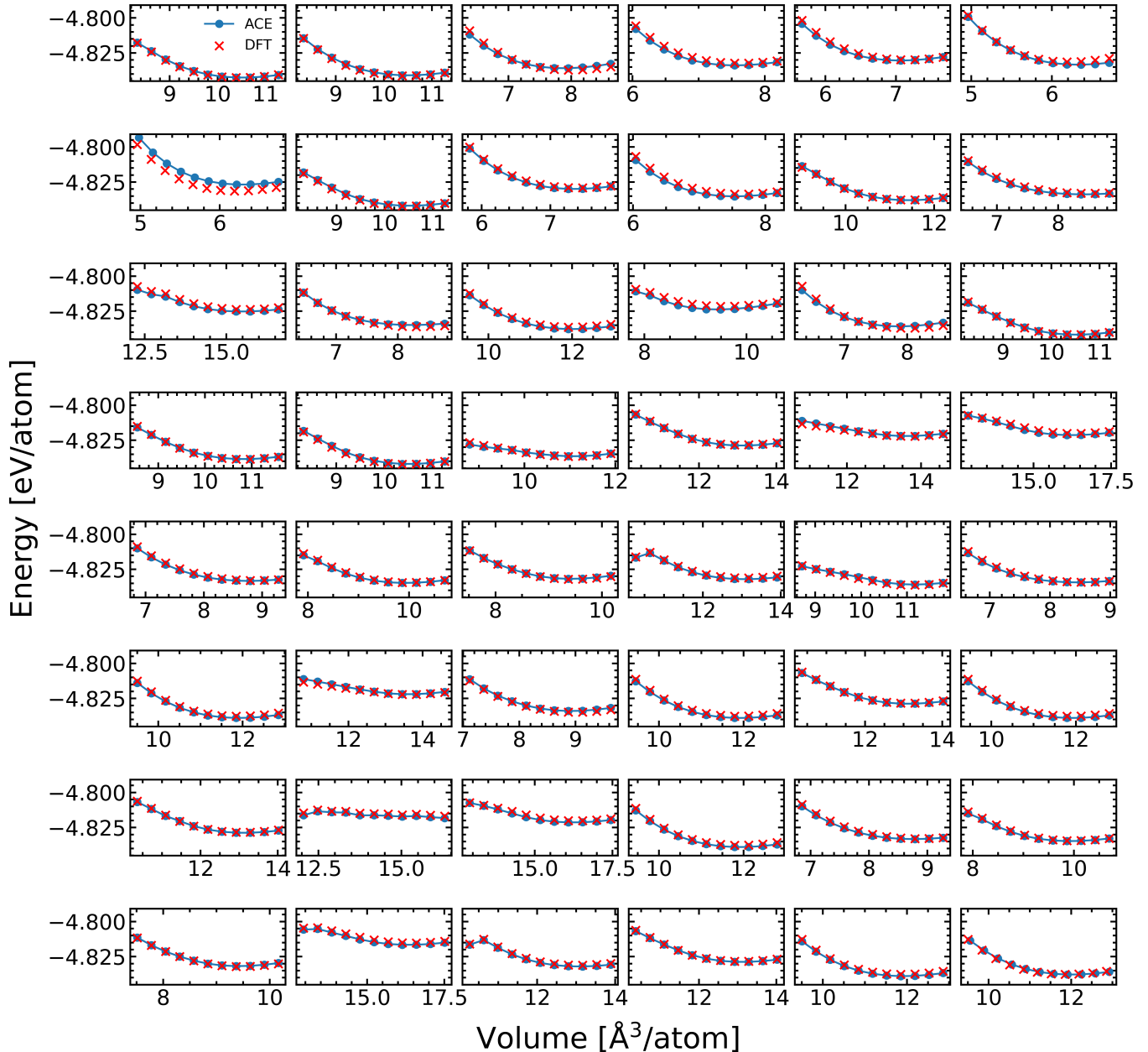


Figure 3: Energy-volume curves for various ice phases in the training dataset. The presented DFT calculations (red crosses) are not part of the training dataset.

3.5 Diffusion coefficient

We calculated the diffusion coefficient for liquid water using two different methods, from Fourier transform of VACF and the mean square displacement (MSD),

$$D = \frac{1}{6} \lim_{t \rightarrow \infty} \frac{d}{dt} \langle |r(t) - r_0|^2 \rangle \quad (2)$$

For MSD, we run 100 independent NVE runs for 100 ps, totalling 10 ns, and for VACF we run 7 independent 100 ps, NVT^{76,77} runs. The

estimated diffusion coefficient shows very good agreement with the DFT reference as well as experimental results,^{18,74,75} where both methods show close agreement, as shown in Table. 2.

Table 2: Computed and experimental diffusion coefficient.

| Method | D [$10^{-9} \text{ m}^2 \text{ s}^{-1}$] | DFT | Experiment ⁷⁸ |
|--------|--|-------------------------------|--------------------------|
| VACF | 2.1 ± 0.02 | 2.22 ± 0.05 ⁷⁴ | 2.41 ± 0.15 |
| MSD | 2.1 ± 0.15 | 1.9 ¹⁸ | |

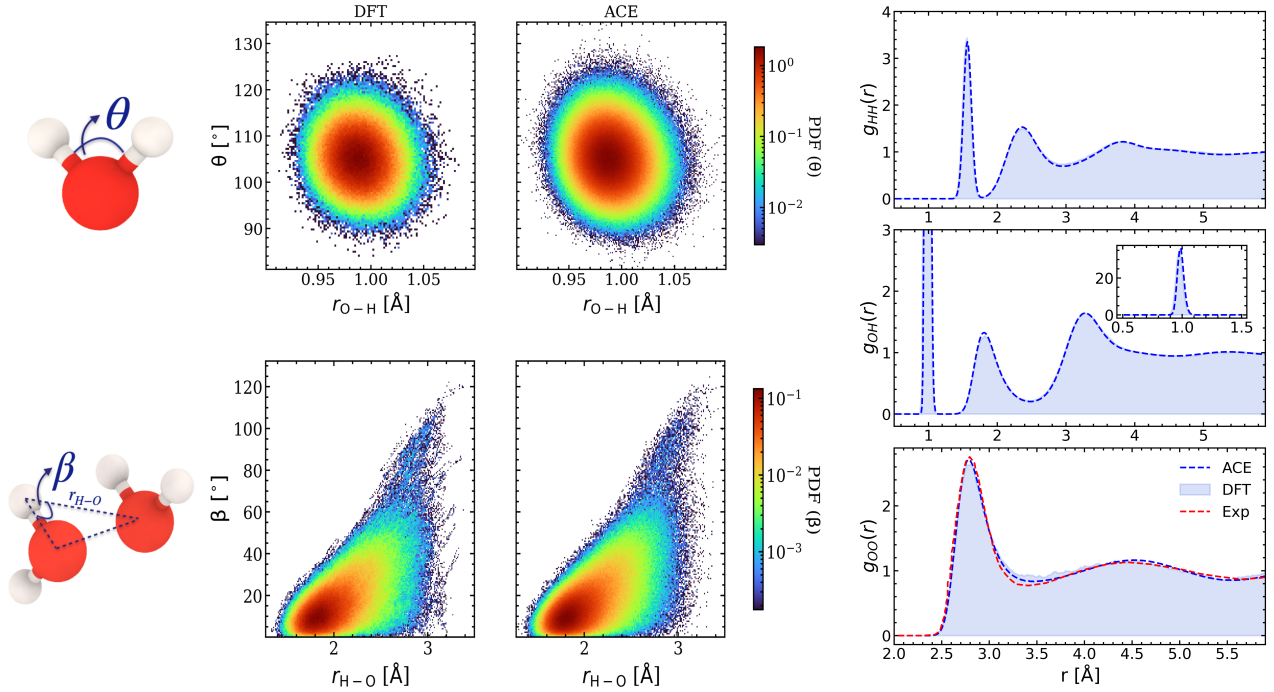


Figure 4: Radial distribution function (right) and the covalent (upper-middle) and hydrogen bonding (lower-middle) profiles in the liquid for DFT and ACE.

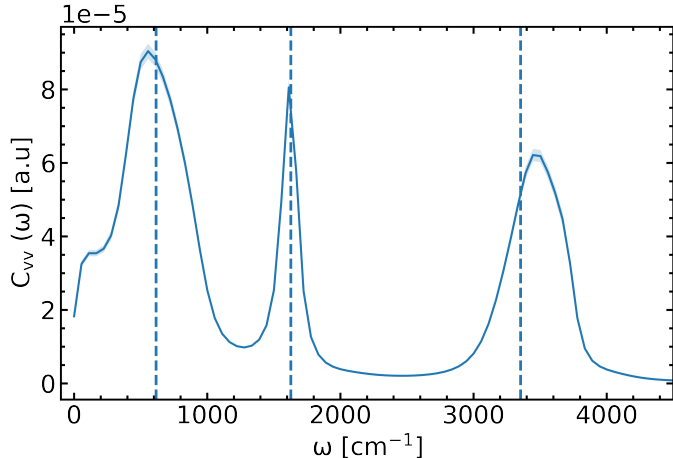


Figure 5: Fourier transform of the velocity auto-correlation function showing the VDOS of our water-ACE potential with peaks corresponding to experimental data ^{44,75} highlighted by vertical lines.

3.6 Melting temperature

We employ coexistence simulations to calculate the melting point of the ice Ih phase. We bring liquid water and ice Ih in contact in a periodic cell with 864 molecules and run NPT simulations at different temperatures in a range of 270 K to 305 K with steps of 5 K at one bar,

where we run each simulation for 5 ns. After this simulation time we observe either complete melting or complete solidification. In Fig. 6, we show the initial and final configurations at each temperature, with complete ice growth below 305 K and complete melting from 305 K and above. We calculate the amount of ice-like molecules using the Auer and Frenke criterion,⁷⁹ implemented in pysical.⁸⁰

3.7 Proton recombination

A key feature of a transferable interatomic potential is its ability to simulate bond breaking and bond formation. Notably, our training dataset excludes configurations with broken bonds.

To test the ability of our ACE to simulate bond formation, we carried out a MD simulation with a water dimer, where one of the molecules had a single broken bond. In an NVT simulation at 300 K we monitored both the energy and the extrapolation grade indicator. As depicted in Fig. 7, our ACE detected significant extrapolation during the initial MD steps, which coincided with relatively high energy states. After several hundred steps,

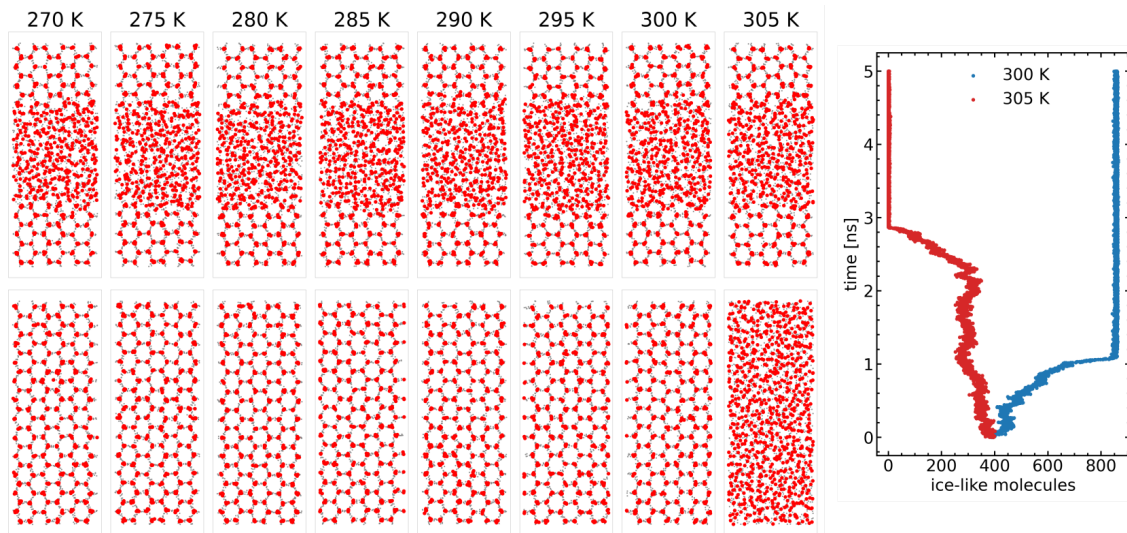


Figure 6: (left panel) Coexistence simulations of liquid water and ice Ih, where we determine the melting point based on complete solidification or complete melting of the interface in a temperature range from 270 K to 305 K with an increment 5 K. The upper row show the initial configurations and the lower row shows the final configurations after 5 ns NPT simulation. (right panel) Number of ice-like-molecules at 300 K and 305 K, where solidification and melting take place, respectively.

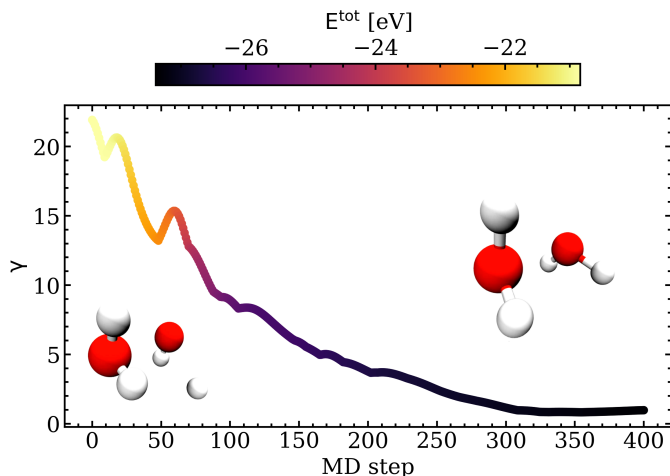


Figure 7: Simulation of proton recombination.

the system stabilized with the detached proton recombining with the water molecule and the extrapolation grade decreased significantly, indicative of reliable and accurate predictions.

4 Conclusion

In this work we introduced a transferable interatomic potential for water using ACE. We followed an efficient sampling methodology for the PES that exploits the similarities of local atomic environments in liquid water and di-

verse ice phases. Therefore, without computationally expensive AIMD simulations, we are able to generate an ACE that shows an excellent match to first-principles computed properties and experiment. We validate the accuracy of our ACE in different applications including energy-volume curves of diverse ice phases, structural analysis including the H-H, O-H, and O-O radial distribution functions as well as the covalent O-H and the non-directional hydrogen bonding profiles, diffusion coefficient, VDOS, melting temperature and proton recombination.

Data availability

The initial ices DFT reference dataset (including ices coordinates) as well as potential files are made available upon acceptance of the manuscript.

Acknowledgements

E.I acknowledges funding through the International Max Planck Research School for Sustainable Metallurgy (IMPRS SusMet). We acknowledge computational resources from the re-

search center ZGH at Ruhr-University Bochum. E.I acknowledges discussion with Christoph Freysoldt.

References

- (1) Jeffrey, G. A.; Jeffrey, G. A. An introduction to hydrogen bonding; Oxford university press New York, 1997; Vol. 12.
- (2) Chaplin, M. F. Structure and properties of water in its various states. Encyclopedia of water: science, technology, and society **2019**, 1–19.
- (3) Monserrat, B.; Brandenburg, J. G.; Engel, E. A.; Cheng, B. Liquid water contains the building blocks of diverse ice phases. Nature communications **2020**, 11, 5757.
- (4) Cheng, B.; Bethkenhagen, M.; Pickard, C. J.; Hamel, S. Phase behaviours of superionic water at planetary conditions. Nature Physics **2021**, 17, 1228–1232.
- (5) Reinhardt, A.; Bethkenhagen, M.; Coppari, F.; Millot, M.; Hamel, S.; Cheng, B. Thermodynamics of high-pressure ice phases explored with atomistic simulations. Nature Communications **2022**, 13, 4707.
- (6) Gartner III, T. E.; Piaggi, P. M.; Car, R.; Panagiotopoulos, A. Z.; Debenedetti, P. G. Liquid-liquid transition in water from first principles. Physical review letters **2022**, 129, 255702.
- (7) Bernal, J. D.; Fowler, R. H. A theory of water and ionic solution, with particular reference to hydrogen and hydroxyl ions. The Journal of Chemical Physics **1933**, 1, 515–548.
- (8) Debenedetti, P. G.; Stanley, H. E. Supercooled and glassy water. Physics Today **2003**, 56, 40–46.
- (9) Coulson, C. A.; Eisenberg, D. Interactions of H₂O molecules in ice I. The dipole moment of an H₂O molecule in ice. Proceedings of the Royal Society of London. Series A. Mathematical and Physical Sciences **1966**, 291, 445–453.
- (10) Batista, E. R.; Xantheas, S. S.; Jónsson, H. Molecular multipole moments of water molecules in ice Ih. The Journal of chemical physics **1998**, 109, 4546–4551.
- (11) Silvestrelli, P. L.; Parrinello, M. Water molecule dipole in the gas and in the liquid phase. Physical Review Letters **1999**, 82, 3308.
- (12) Badyal, Y.; Saboungi, M.-L.; Price, D.; Shastri, S.; Haefner, D.; Soper, A. Electron distribution in water. The Journal of Chemical Physics **2000**, 112, 9206–9208.
- (13) Gillan, M. J.; Alfe, D.; Michaelides, A. Perspective: How good is DFT for water? The Journal of chemical physics **2016**, 144, 130901.
- (14) Cisneros, G. A.; Wikfeldt, K. T.; Ojamaäe, L.; Lu, J.; Xu, Y.; Torabifard, H.; Bartók, A. P.; Csányi, G.; Molinero, V.; Paesani, F. Modeling molecular interactions in water: From pairwise to many-body potential energy functions. Chemical reviews **2016**, 116, 7501–7528.
- (15) Medders, G. R.; Babin, V.; Paesani, F. A critical assessment of two-body and three-body interactions in water. Journal of chemical theory and computation **2013**, 9, 1103–1114.
- (16) Laasonen, K.; Sprik, M.; Parrinello, M.; Car, R. “Ab initio” liquid water. The Journal of chemical physics **1993**, 99, 9080–9089.
- (17) Tuckerman, M.; Laasonen, K.; Sprik, M.; Parrinello, M. Ab initio simulations of water and water ions. Journal of Physics: Condensed Matter **1994**, 6, A93.

- (18) Pestana, L. R.; Mardirossian, N.; Head-Gordon, M.; Head-Gordon, T. Ab initio molecular dynamics simulations of liquid water using high quality meta-GGA functionals. Chemical science **2017**, 8, 3554–3565.
- (19) Ruiz Pestana, L.; Marsalek, O.; Markland, T. E.; Head-Gordon, T. The quest for accurate liquid water properties from first principles. The journal of physical chemistry letters **2018**, 9, 5009–5016.
- (20) Chen, M.; Ko, H.-Y.; Remsing, R. C.; Calegari Andrade, M. F.; Santra, B.; Sun, Z.; Selloni, A.; Car, R.; Klein, M. L.; Perdew, J. P.; others Ab initio theory and modeling of water. Proceedings of the National Academy of Sciences **2017**, 114, 10846–10851.
- (21) Sun, J.; Ruzsinszky, A.; Perdew, J. P. Strongly constrained and appropriately normed semilocal density functional. Physical review letters **2015**, 115, 036402.
- (22) Sun, J.; Remsing, R. C.; Zhang, Y.; Sun, Z.; Ruzsinszky, A.; Peng, H.; Yang, Z.; Paul, A.; Waghmare, U.; Wu, X.; others Accurate first-principles structures and energies of diversely bonded systems from an efficient density functional. Nature chemistry **2016**, 8, 831–836.
- (23) Sprik, M.; Hutter, J.; Parrinello, M. Ab initio molecular dynamics simulation of liquid water: Comparison of three gradient-corrected density functionals. The Journal of chemical physics **1996**, 105, 1142–1152.
- (24) Errington, J. R.; Debenedetti, P. G. Relationship between structural order and the anomalies of liquid water. Nature **2001**, 409, 318–321.
- (25) Krack, M.; Gambirasio, A.; Parrinello, M. Ab initio x-ray scattering of liquid water. The Journal of chemical physics **2002**, 117, 9409–9412.
- (26) Sharma, M.; Resta, R.; Car, R. Inter-molecular dynamical charge fluctuations in water: A signature of the H-bond network. Physical review letters **2005**, 95, 187401.
- (27) Zhang, C.; Donadio, D.; Gygi, F.; Galli, G. First principles simulations of the infrared spectrum of liquid water using hybrid density functionals. Journal of chemical theory and computation **2011**, 7, 1443–1449.
- (28) Herbert, J. M. Structure of the aqueous electron. Physical Chemistry Chemical Physics **2019**, 21, 20538–20565.
- (29) Svoboda, V.; Michiels, R.; LaForge, A. C.; Stienkemeier, F.; Slavíček, P.; Wörner, H. J. Real-time observation of water radiolysis and hydrated electron formation induced by extreme-ultraviolet pulses. Science Advances **2020**, 6, eaaz0385.
- (30) Nishitani, J.; Yamamoto, Y.-i.; West, C. W.; Karashima, S.; Suzuki, T. Binding energy of solvated electrons and retrieval of true UV photoelectron spectra of liquids. Science Advances **2019**, 5, eaaw6896.
- (31) Turi, L.; Sheu, W.-S.; Rossky, P. J. Characterization of excess electrons in water-cluster anions by quantum simulations. Science **2005**, 309, 914–917.
- (32) Savolainen, J.; Uhlig, F.; Ahmed, S.; Hamm, P.; Jungwirth, P. Direct observation of the collapse of the delocalized excess electron in water. Nature chemistry **2014**, 6, 697–701.
- (33) Gartmann, T. E.; Ban, L.; Yoder, B. L.; Hartweg, S.; Chasovskikh, E.; Signorell, R. Relaxation dynamics and genuine properties of the solvated electron in neutral water clusters. The Journal of Physical Chemistry Letters **2019**, 10, 4777–4782.

- (34) MacKerell Jr, A. D.; Bashford, D.; Bellott, M.; Dunbrack Jr, R. L.; Evanseck, J. D.; Field, M. J.; Fischer, S.; Gao, J.; Guo, H.; Ha, S.; others All-atom empirical potential for molecular modeling and dynamics studies of proteins. The journal of physical chemistry B **1998**, 102, 3586–3616.
- (35) Jorgensen, W. L.; Chandrasekhar, J.; Madura, J. D.; Impey, R. W.; Klein, M. L. Comparison of simple potential functions for simulating liquid water. The Journal of chemical physics **1983**, 79, 926–935.
- (36) Price, D. J.; Brooks, C. L. A modified TIP3P water potential for simulation with Ewald summation. The Journal of chemical physics **2004**, 121, 10096–10103.
- (37) Abascal, J. L.; Vega, C. A general purpose model for the condensed phases of water: TIP4P/2005. The Journal of chemical physics **2005**, 123, 234505.
- (38) Bartók, A. P.; De, S.; Poelking, C.; Bernstein, N.; Kermode, J. R.; Csányi, G.; Ceriotti, M. Machine learning unifies the modeling of materials and molecules. Science advances **2017**, 3, e1701816.
- (39) Kulik, H.; Hammerschmidt, T.; Schmidt, J.; Botti, S.; Marques, M.; Boley, M.; Scheffler, M.; Todorović, M.; Rinke, P.; Oses, C.; others Roadmap on machine learning in electronic structure. Electronic Structure **2022**, 4, 023004.
- (40) Deringer, V. L.; Bartók, A. P.; Bernstein, N.; Wilkins, D. M.; Ceriotti, M.; Csányi, G. Gaussian process regression for materials and molecules. Chemical Reviews **2021**, 121, 10073–10141.
- (41) Cheng, B.; Engel, E. A.; Behler, J.; Delgado, C.; Ceriotti, M. Ab initio thermodynamics of liquid and solid water. Proceedings of the National Academy of Sciences **2019**, 116, 1110–1115.
- (42) Lan, J.; Kapil, V.; Gasparotto, P.; Ceriotti, M.; Iannuzzi, M.; Rybkin, V. V. Simulating the ghost: quantum dynamics of the solvated electron. Nature communications **2021**, 12, 766.
- (43) Daru, J.; Forbert, H.; Behler, J.; Marx, D. Coupled cluster molecular dynamics of condensed phase systems enabled by machine learning potentials: Liquid water benchmark. Physical Review Letters **2022**, 129, 226001.
- (44) Liu, J.; Lan, J.; He, X. Toward High-level Machine Learning Potential for Water Based on Quantum Fragmentation and Neural Networks. The Journal of Physical Chemistry A **2022**, 126, 3926–3936.
- (45) Piaggi, P. M.; Panagiotopoulos, A. Z.; Debenedetti, P. G.; Car, R. Phase equilibrium of water with hexagonal and cubic ice using the scan functional. Journal of Chemical Theory and Computation **2021**, 17, 3065–3077.
- (46) Kapil, V.; Kovács, D. P.; Csányi, G.; Michaelides, A. First-principles spectroscopy of aqueous interfaces using machine-learned electronic and quantum nuclear effects. Faraday Discussions **2024**,
- (47) Reinhardt, A.; Cheng, B. Quantum-mechanical exploration of the phase diagram of water. Nature communications **2021**, 12, 588.
- (48) Schran, C.; Thiemann, F. L.; Rowe, P.; Müller, E. A.; Marsalek, O.; Michaelides, A. Machine learning potentials for complex aqueous systems made simple. Proceedings of the National Academy of Sciences **2021**, 118, e2110077118.
- (49) Kresse, G. Google Scholar Crossref, ISI G. Kresse and J. Hafner. Phys. Rev. B <https://doi.org/10.1103/PhysRevB.1994.49>, 14251.
- (50) Kresse, G.; Furthmüller, J. Efficiency of ab-initio total energy calculations for metals and semiconductors using a plane-wave

- basis set. Computational materials science **1996**, 6, 15–50.
- (51) Kresse, G.; Furthmüller, J. Efficient iterative schemes for ab initio total-energy calculations using a plane-wave basis set. Physical review B **1996**, 54, 11169.
- (52) Perdew, J. P.; Burke, K.; Ernzerhof, M. Generalized gradient approximation made simple. Physical review letters **1996**, 77, 3865.
- (53) Grimme, S.; Antony, J.; Ehrlich, S.; Krieg, H. A consistent and accurate ab initio parametrization of density functional dispersion correction (DFT-D) for the 94 elements H-Pu. The Journal of chemical physics **2010**, 132, 154104.
- (54) Grimme, S.; Ehrlich, S.; Goerigk, L. Effect of the damping function in dispersion corrected density functional theory. Journal of computational chemistry **2011**, 32, 1456–1465.
- (55) Thompson, A. P.; Aktulga, H. M.; Berger, R.; Bolintineanu, D. S.; Brown, W. M.; Crozier, P. S.; in 't Veld, P. J.; Kohlmeyer, A.; Moore, S. G.; Nguyen, T. D.; Shan, R.; Stevens, M. J.; Tranchida, J.; Trott, C.; Plimpton, S. J. LAMMPS - a flexible simulation tool for particle-based materials modeling at the atomic, meso, and continuum scales. Comp. Phys. Comm. **2022**, 271, 108171.
- (56) Lysogorskiy, Y.; Oord, C. v. d.; Bochkarev, A.; Menon, S.; Rinaldi, M.; Hammerschmidt, T.; Mrovec, M.; Thompson, A.; Csányi, G.; Ortner, C.; others Performant implementation of the atomic cluster expansion (PACE) and application to copper and silicon. npj computational materials **2021**, 7, 97.
- (57) Kapil, V.; Rossi, M.; Marsalek, O.; Petraglia, R.; Litman, Y.; Spura, T.; Cheng, B.; Cuzzocrea, A.; Meißner, R. H.; Wilkins, D. M.; others i-PI 2.0: A universal force engine for advanced molecular simulations. Computer Physics Communications **2019**, 236, 214–223.
- (58) Drautz, R. Atomic cluster expansion for accurate and transferable interatomic potentials. Physical Review B **2019**, 99, 014104.
- (59) Dusson, G.; Bachmayr, M.; Csányi, G.; Drautz, R.; Etter, S.; van der Oord, C.; Ortner, C. Atomic cluster expansion: Completeness, efficiency and stability. Journal of Computational Physics **2022**, 454, 110946.
- (60) Bochkarev, A.; Lysogorskiy, Y.; Menon, S.; Qamar, M.; Mrovec, M.; Drautz, R. Efficient parametrization of the atomic cluster expansion. Physical Review Materials **2022**, 6, 013804.
- (61) Ibrahim, E.; Lysogorskiy, Y.; Mrovec, M.; Drautz, R. Atomic cluster expansion for a general-purpose interatomic potential of magnesium. Phys. Rev. Mater. **2023**, 7, 113801.
- (62) Qamar, M.; Mrovec, M.; Lysogorskiy, Y.; Bochkarev, A.; Drautz, R. Atomic cluster expansion for quantum-accurate large-scale simulations of carbon. Journal of Chemical Theory and Computation **2023**, 19, 5151–5167.
- (63) Bochkarev, A.; Lysogorskiy, Y.; Ortner, C.; Csányi, G.; Drautz, R. Multi-layer atomic cluster expansion for semilocal interactions. Physical Review Research **2022**, 4, L042019.
- (64) Rinaldi, M.; Mrovec, M.; Bochkarev, A.; Lysogorskiy, Y.; Drautz, R. Non-collinear magnetic atomic cluster expansion for iron. npj Computational Materials **2024**, 10, 12.
- (65) Bochkarev, A.; Lysogorskiy, Y.; Drautz, R. Atomic Cluster Expansion for semilocal interactions beyond equivariant message passing. arXiv preprint arXiv:2311.16326 **2023**,

- (66) Bochkarev, A.; Lysogorskiy, Y.; Drautz, R. Graph Atomic Cluster Expansion for Semilocal Interactions beyond Equivariant Message Passing. Physical Review X **2024**, 14, 021036.
- (67) Matsumoto, M.; Yagasaki, T.; Tanaka, H. GenIce: Hydrogen-Disordered Ice Generator. Journal of Computational Chemistry **2017**, 39, 61–64.
- (68) Matsumoto, M.; Yagasaki, T.; Tanaka, H. Novel Algorithm to Generate Hydrogen-Disordered Ice Structures. Journal of Chemical Information and Modeling **2021**, 61, 2542–2546.
- (69) Lysogorskiy, Y.; Bochkarev, A.; Mrovec, M.; Drautz, R. Active learning strategies for atomic cluster expansion models. Physical Review Materials **2023**, 7, 043801.
- (70) LJPvd, M.; Hinton, G. Visualizing high-dimensional data using t-SNE. J Mach Learn Res **2008**, 9, 9.
- (71) Belkina, A. C.; Ciccolella, C. O.; Anno, R.; Halpert, R.; Spidlen, J.; Snyder-Cappione, J. E. Automated optimized parameters for T-distributed stochastic neighbor embedding improve visualization and analysis of large datasets. Nature communications **2019**, 10, 5415.
- (72) Pedregosa, F.; Varoquaux, G.; Gramfort, A.; Michel, V.; Thirion, B.; Grisel, O.; Blondel, M.; Prettenhofer, P.; Weiss, R.; Dubourg, V.; Vanderplas, J.; Passos, A.; Cournapeau, D.; Brucher, M.; Perrot, M.; Duchesnay, E. Scikit-learn: Machine Learning in Python. Journal of Machine Learning Research **2011**, 12, 2825–2830.
- (73) Janssen, J.; Surendralal, S.; Lysogorskiy, Y.; Todorova, M.; Hickel, T.; Drautz, R.; Neugebauer, J. pyiron: An integrated development environment for computational materials science. Computational Materials Science **2019**, 163, 24–36.
- (74) Marsalek, O.; Markland, T. E. Quantum dynamics and spectroscopy of ab initio liquid water: The interplay of nuclear and electronic quantum effects. The journal of physical chemistry letters **2017**, 8, 1545–1551.
- (75) Yao, Y.; Kanai, Y. Nuclear quantum effect and its temperature dependence in liquid water from random phase approximation via artificial neural network. The journal of physical chemistry letters **2021**, 12, 6354–6362.
- (76) Nosé, S. A unified formulation of the constant temperature molecular dynamics methods. The Journal of chemical physics **1984**, 81, 511–519.
- (77) Hoover, W. G. Canonical dynamics: Equilibrium phase-space distributions. Physical review A **1985**, 31, 1695.
- (78) Skinner, L. B.; Huang, C.; Schlesinger, D.; Pettersson, L. G.; Nilsson, A.; Benmore, C. J. Benchmark oxygen-oxygen pair-distribution function of ambient water from x-ray diffraction measurements with a wide Q-range. The Journal of chemical physics **2013**, 138.
- (79) Auer, S.; Frenkel, D. Numerical simulation of crystal nucleation in colloids. Advanced Computer Simulation: Approaches for Soft Matter Sciences I **2005**, 149–208.
- (80) Menon, S.; Leines, G. D.; Rogal, J. pycal: A python module for structural analysis of atomic environments. Journal of Open Source Software **2019**, 4, 1824.